

# Steatohepatitis, Spontaneous Peroxisome Proliferation and Liver Tumors in Mice Lacking Peroxisomal Fatty Acyl-CoA Oxidase

IMPLICATIONS FOR PEROXISOME PROLIFERATOR-ACTIVATED RECEPTOR  $\alpha$  NATURAL LIGAND METABOLISM\*

(Received for publication, February 10, 1998, and in revised form, March 27, 1998)

Chun-Yang Fan<sup>‡</sup>, Jie Pan<sup>‡</sup>, Nobuteru Usuda, Anjana V. Yeldandi, M. Sambasiva Rao, and Janardan K. Reddy<sup>§</sup>

From the Department of Pathology, Northwestern University Medical School, Chicago, Illinois 60611-3008

**Peroxisomal  $\beta$ -oxidation system consists of four consecutive reactions to preferentially metabolize very long chain fatty acids. The first step of this system, catalyzed by acyl-CoA oxidase (AOX), converts fatty acyl-CoA to 2-trans-enoyl-CoA. Herein, we show that mice deficient in AOX exhibit steatohepatitis, increased hepatic  $H_2O_2$  levels, and hepatocellular regeneration, leading to a complete reversal of fatty change by 6 to 8 months of age. The liver of AOX<sup>-/-</sup> mice with regenerated hepatocytes displays profound generalized spontaneous peroxisome proliferation and increased mRNA levels of genes that are regulated by peroxisome proliferator-activated receptor  $\alpha$  (PPAR $\alpha$ ). Hepatic adenomas and carcinomas develop in AOX<sup>-/-</sup> mice by 15 months of age due to sustained activation of PPAR $\alpha$ . These observations implicate acyl-CoA and other putative substrates for AOX, as biological ligands for PPAR $\alpha$ ; thus, a normal AOX gene is indispensable for the physiological regulation of PPAR $\alpha$ .**

Peroxisomes are single membrane-bound organelles present in most eukaryotic cells. They participate in a variety of metabolic processes such as lipid metabolism,  $H_2O_2$ -based respiration, production of bile acids and plasmalogens (membrane phospholipids), synthesis of cholesterol, and catabolism of purines, polyamines, and amino acids (1–3). Peroxisomes in liver parenchymal cells can be stimulated to proliferate by the administration of nonmutagenic chemicals designated as peroxisome proliferators (4). These include certain phthalate ester plasticizers, industrial solvents, herbicides, leukotriene D<sub>4</sub> antagonists, the adrenal steroid dehydroepiandrosterone, as well as amphipathic carboxylates such as the hypolipidemic drugs, clofibrate, and ciprofibrate (5). Peroxisome proliferation induced by these structurally diverse agents is associated with transcriptional activation of genes encoding for the peroxisomal  $\beta$ -oxidation system (6, 7) and the cytochrome P450 CYP4A isoforms (8), among others (9, 10). The induction of peroxisome proliferation is mediated by peroxisome proliferator-activated

receptors (PPARs)<sup>1</sup> that form a complex with the common heterodimeric partner, retinoid X receptor (RXR) (11, 12). The PPAR-RXR complex binds to peroxisome proliferator-responsive element (PPRE), a region consisting of a degenerate direct repeat of the canonical AGGTCA sequence separated by 1 base pair (DR1), present in the 5'-flanking region of target genes (9, 10, 12). Three isotypes of PPARs, namely PPAR $\alpha$ , PPAR $\delta$  (also known as PPAR $\beta$ , NUC-1), and PPAR $\gamma$ , have been identified as products of separate genes from *Xenopus*, rodents and humans (11, 13–16). These isotypes exhibit distinct patterns of tissue distribution and differ considerably in their ligand binding domains, suggesting that they possibly perform different functions in different cell types (15–24). Indeed, of the three isotypes, PPAR $\alpha$  expression is relatively high in hepatocytes, enterocytes, and the proximal convoluted tubular epithelium of kidney (17, 18), and evidence derived from mice with PPAR $\alpha$  gene disruption indicates that this receptor is essential for the pleiotropic responses induced by peroxisome proliferators (25).

Sustained induction of PPAR $\alpha$ -mediated peroxisome proliferation leads to the development of liver tumors in rats and mice exposed chronically to peroxisome proliferators despite their nonmutagenic nature (5, 26). It has been postulated that  $H_2O_2$  overproduced by the sustained transcriptional activation of peroxisomal  $\beta$ -oxidation system and concomitant cell proliferation contribute to hepatocarcinogenesis in livers with peroxisome proliferation (5, 26–29). The peroxisomal  $\beta$ -oxidation system consists of three enzymes, namely  $H_2O_2$ -generating fatty acyl-CoA oxidase (AOX), enoyl-CoA hydratase/3-hydroxyacyl-CoA dehydrogenase multifunctional protein (MFP), and 3-ketoacyl-CoA thiolase (THL) (3, 6, 30). Although peroxisomes and mitochondria catalyze similar reactions, the long chain and very long chain fatty acids (VLCFAs) are oxidized predominantly, if not exclusively, by the peroxisomal  $\beta$ -oxidation system (3, 30–32). To investigate the role of peroxisomal  $\beta$ -oxidation in hepatocarcinogenesis and to assess the long range implications of disturbing VLCFA metabolism, we generated an animal model of AOX deficiency by inactivating the gene encoding the AOX (33, 34), the first enzyme of the peroxisomal  $\beta$ -oxidation system, which converts acyl-CoA to enoyl-

\* This work was supported by National Institutes of Health Grant GM 23750 (to J. K. R.), Veterans Affairs merit review grants (to A. V. Y. and M. S. R.), Joseph L. Mayberry, Sr. Endowment Fund, and the Adrian Mayer, M. D., Cancer Research Fund. The costs of publication of this article were defrayed in part by the payment of page charges. This article must therefore be hereby marked "advertisement" in accordance with 18 U.S.C. Section 1734 solely to indicate this fact.

<sup>‡</sup> These authors contributed equally to this work.

<sup>§</sup> To whom correspondence should be addressed: Dept. of Pathology, Northwestern University of Medical School, 303 East Chicago Ave., Chicago, IL 60611-3008. Tel.: 312-503-7948; Fax: 312 503 8249; E-mail: jkreddy@nwu.edu.

<sup>1</sup> The abbreviations used are: PPAR, peroxisome proliferator-activated receptor; AOX, fatty acyl-CoA oxidase; PPRE, peroxisome proliferator response element; RXR, retinoid-x-receptor for 9-*cis*-retinoic acid; MFP, enoyl-CoA hydratase/3-hydroxyacyl-CoA dehydrogenase multifunctional protein; THL, 3-ketoacyl-CoA thiolase; VLCFA, long-chain and very-long chain fatty acid; PCNA, proliferating cell nuclear antigen; PMP70, 70-kDa peroxisomal membrane protein; UOX, urate oxidase; FABP, fatty acid-binding protein; ACS, fatty acyl-CoA synthetase; FAS, fatty acid synthetase; X-ALD, X-linked adrenoleukodystrophy; CYP4A1 and CYP4A3, encode microsomal cytochrome P450 fatty acid  $\omega$ -hydroxylases.

CoA (30). Analysis of young AOX-deficient mice revealed extensive microvesicular fatty metamorphosis of liver parenchymal cells and inflammatory reaction (34). Hepatic steatosis begins to dissipate gradually, resulting in a liver consisting entirely of regenerative hepatocytes that display massive spontaneous peroxisome proliferation indicative of PPAR $\alpha$  activation. Liver tumors develop in AOX-deficient mice by 15 months of age. Our findings implicate AOX as a key regulator of PPAR $\alpha$  function and acyl-CoAs (other possible natural substrates of AOX) as potent biological ligands responsible for the transcriptional activation of PPAR $\alpha$  *in vivo*.

#### EXPERIMENTAL PROCEDURES

**Animals**—We utilized the fatty acyl-CoA oxidase null (AOX $-/-$ ) mice as described (34). Heterozygous (AOX $\pm$ ) siblings were mated to obtain AOX $-/-$  mice because of reduced fertility of homozygous males and females (34). Genotypes of mice were determined by Southern blot analysis using DNA isolated from tail tip (34). Age-matched wild-type (AOX $+/+$ ) siblings served as controls as needed. Animal care and experiments were carried out in accordance with both institutional and federal animal care regulations.

**Histology and Immunohistology**—For routine histology, tissues were fixed in 10% phosphate-buffered formalin (pH 7.4) dehydrated in 100% ethanol and embedded in paraffin at 58 °C using standard procedures. Sections (4  $\mu$ m thick) were cut and stained with hematoxylin and eosin. For immunohistochemical localization of AOX, MFP, THL, catalase, and proliferating cell nuclear antigen (PCNA), tissues fixed in 10% formalin or 70% ethanol were processed using monospecific polyclonal antibodies. Immunostaining was performed by an avidin-biotinylated peroxidase complex (ABC kit, Vector Laboratories) or by the peroxidase-anti-peroxidase method. Negative controls consisted of staining with normal rabbit serum instead of specific antibodies or by omitting the primary antibodies. The slides were counterstained with either hematoxylin or methyl green.

**Electron Microscopy and Immunocytochemistry**—For routine transmission electron microscopy, samples of liver were fixed with 2% paraformaldehyde and 2.5% glutaraldehyde in 0.05 M cacodylate buffer (pH 7.2, 4 °C) for 4 h. They were washed overnight in cacodylate buffer, post-fixed in 1% osmium tetroxide in cacodylate buffer (pH 7.4) for 1 h at 4 °C, and embedded in Epon. For cytochemical localization of catalase, tissue samples were fixed in 1.5% glutaraldehyde in 0.1 M sodium cacodylate buffer (pH 7.4) for 4 h at 4 °C, washed overnight with 0.1% cacodylate buffer (pH 7.4), and cut into 60- $\mu$ m sections. The sections were stained for catalase with alkaline 3,3'-diaminobenzidine substrate and post-fixed with 1% osmium tetroxide in 0.1 M cacodylate buffer (pH 7.4). Semithin sections with or without toluidine blue counterstain were examined by light microscopy. Ultrathin sections for electron microscopy were contrasted with uranyl acetate and lead citrate. For immunogold localization of AOX, MFP, THL, and urate oxidase, tissues were fixed for 24 h by immersion in 4% paraformaldehyde, 0.1% glutaraldehyde in 0.1 M sodium phosphate buffer (pH 7.4) at 4 °C. The sections were rinsed for 3 h in 0.1 M sodium phosphate, pH 7.4, 0.15 M NaCl, 0.1 M lysine, dehydrated in graded series of cold ethanol, and embedded in Lowicryl K4M at -20 °C. Ultrathin sections were stained with each antibody by the protein A-gold technique. The polyclonal antibodies used in these studies were raised in rabbits against rat catalase, rat AOX, rat MFP, rat THL, and rat urate oxidase (35).

**Northern Blots**—Total cellular RNA was isolated from fresh liver or liver frozen at -80 °C using the acid guanidinium thiocyanate-phenol-chloroform extraction method. RNA was glyoxylated, separated on 0.8% agarose gel, and transferred to a nylon membrane. cDNA probes used for Northern blotting included AOX, catalase MFP, THL, 70-kDa peroxisomal membrane protein (PMP70), urate oxidase (UOX), CYP4A1, CYP4A3, liver FAPB, fatty acid synthase (FAS), fatty acyl-CoA synthetase (ACS), and ribosomal RNA (28 S). Changes in mRNA levels were estimated by densitometric scanning of autoradiograms.

**H<sub>2</sub>O<sub>2</sub> Measurement**—Samples of liver were homogenized (1% w/v) in lysis buffer (0.2 M Tris-HCl, pH 8.0, 0.1 M EDTA, 2% SDS containing 20 mM NaN<sub>3</sub> to inhibit endogenous catalase), and H<sub>2</sub>O<sub>2</sub> was measured using the phenol red method (36).

#### RESULTS

**Histological Changes in Liver of AOX $-/-$  Mice**—Information on the generation of AOX $-/-$  mice has been presented previously (34). Homozygous AOX $-/-$  mice lacked the expression of AOX protein, accumulated VLCFAs in blood, and exhib-

ited growth retardation during the first six months of age when compared with wild-type (AOX $+/+$ ) littermates (34). Both male and female AOX $-/-$  mice at four months are infertile, possibly due to retarded growth and development (34). For this study, homozygous (AOX $-/-$ ) animals were obtained by mating heterozygous (AOX $\pm$ ) mice. At 2 months of age, AOX $-/-$  mice exhibited severe and diffuse fatty metamorphosis of liver, reflecting acute fatty acid hepatotoxicity in younger animals. Scattered hepatocyte death and numerous foci of steatohepatitis are encountered during the first 4 months of age (Fig. 1A). During the first 2 to 4 months of age, the inflammatory response consisted mostly of polymorphonuclear neutrophils, lipogranulomas, and clusters of foamy macrophages. Death of single hepatocytes (apoptosis) and inflammatory response served as stimuli for progressive liver cell regeneration, resulting in the appearance of multiple clusters of hepatocytes with hypertrophic granular cytoplasm. These regenerated hepatocytes are resistant to fatty change and contained no lipid vacuoles. Few cells with fatty change are sometimes present at the periphery of these newly formed regenerating hepatocyte foci. As the regeneration extended, eosinophilic hepatocyte foci coalesced to form confluent areas of liver regeneration. Thus, between 6 and 8 months of age, almost all steatotic hepatocytes in AOX $-/-$  mice were replaced by hepatocytes devoid of steatosis (Fig. 1B). Few areas of inflammatory cell collections and large lipid-laden macrophages, some of which are multinucleated, are seen as remnants in a liver that was once steatotic (Fig. 1B, arrows).

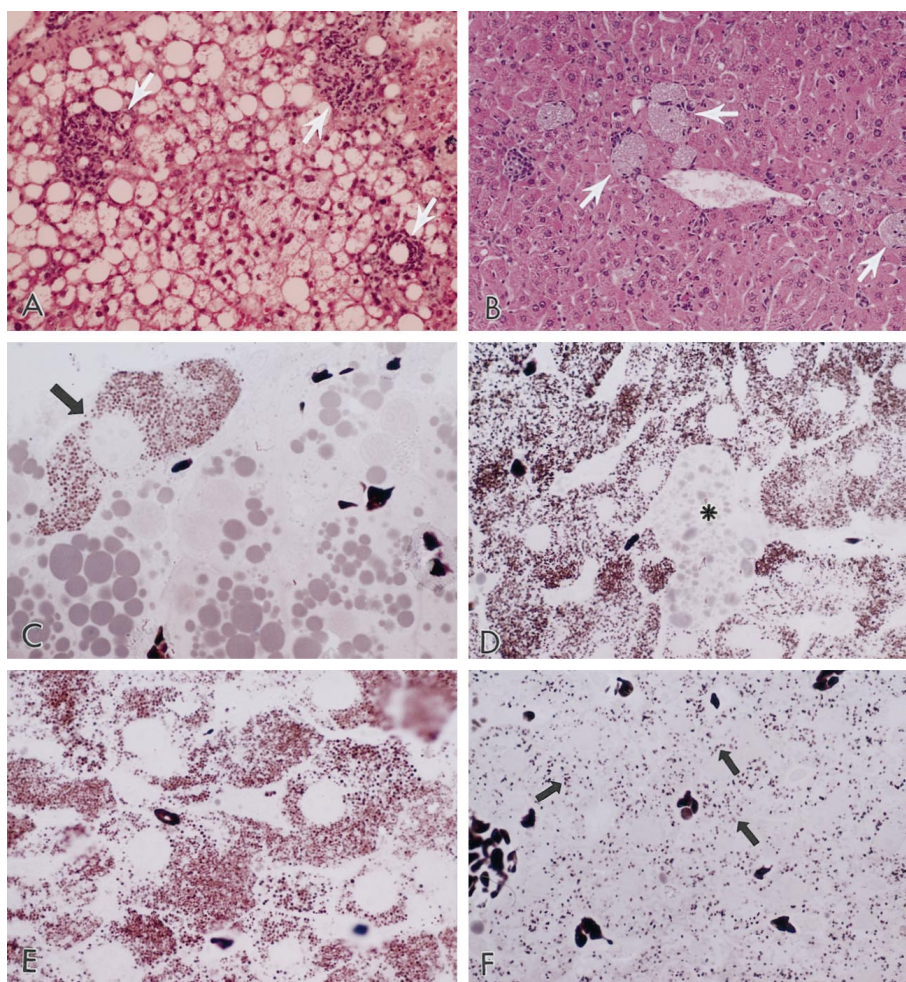
**Spontaneous Hepatic Peroxisome Proliferation**—Peroxisomes can be identified at the light microscopic level in cytochemically stained sections by the alkaline 3,3'-diaminobenzidine procedure for the peroxisomal marker enzyme catalase (1). In hepatocytes of AOX $+/+$  mice, peroxisomes are few, randomly distributed in the cytoplasm, and appeared as diaminobenzidine positive, dark brown granules (Fig. 1F). Evaluation of 2- to 4-month-old AOX $-/-$  mice revealed a conspicuous absence or paucity of recognizable diaminobenzidine-positive organelles in diffusely steatotic hepatocytes (Fig. 1C). Since steatosis is extensive in young AOX $-/-$  mice, recognizable peroxisomes are found only in a rare hepatocyte. An occasional hepatocyte with no fatty change displayed an abundance of peroxisomes (Fig. 1C). As hepatocellular regeneration ensued, the number of hepatocytes lacking steatosis increased, and such cells exhibited conspicuous peroxisome proliferation. As steatosis dissipated in animals six months and older, repopulation of liver occurred with hepatocytes containing eosinophilic cytoplasm (Fig. 1B). These cells displayed massive spontaneous peroxisome proliferation (Fig. 1, D and E). Ultrastructural analysis of the liver of AOX $-/-$  mice confirmed the increase in the number of peroxisomes in hepatic parenchymal cells (Fig. 2). The magnitude of peroxisome proliferation encountered in these AOX-deficient mice is comparable with that induced in wild-type mice by exogenous peroxisome proliferators such as hypolipidemic drugs Wy-14,643, clofibrate, and ciprofibrate (4, 5). Many peroxisomes in hepatocytes of AOX $-/-$  mice revealed the presence of prominent UOX-containing crystalloid cores (Fig. 2A).

**Up-regulation of PPAR $\alpha$  Target Genes**—PPAR $\alpha$  plays a crucial role in the peroxisome proliferation induced in liver by peroxisome proliferators such as clofibrate and Wy-14,643 (25, 37). Mice deficient in PPAR $\alpha$  (PPAR $\alpha$  $-/-$ ) contain a normal complement of peroxisomes in liver parenchymal cells, but these animals do not exhibit the typical predictable pleiotropic responses, including the development of liver tumors, when treated with peroxisome proliferators (25, 37). The massive spontaneous peroxisome proliferation observed in AOX-deficient mice in the present study is reminiscent of that encountered in mice exposed to potent peroxisome proliferators such



**FIG. 1. Hepatocellular alterations in liver of AOX<sup>-/-</sup> mice.**

The liver of a 3-month-old (A) and an 8-month-old (B) AOX<sup>-/-</sup> mouse stained with hematoxylin-eosin. Fatty metamorphosis of hepatocytes and aggregates of inflammatory cells (arrows) are common in young AOX-deficient mice (A). In older AOX<sup>-/-</sup> mice, liver is composed predominantly of cells with abundant eosinophilic granular cytoplasm with few large foamy lipid-laden macrophages (arrows) and residual inflammation (B). C-F, light microscopic appearance of liver as revealed in semi-thin sections of tissues that were processed for the cytochemical localization of peroxisomal catalase using the alkaline 3,3'-diaminobenzidine substrate. These sections are intended to demonstrate the magnitude of spontaneous peroxisome proliferation in the liver parenchymal cells of older AOX<sup>-/-</sup> mice. C, liver of a 3-month-old AOX<sup>-/-</sup> mouse similar to that in (A) shows a single cell (arrow) with numerous peroxisomes (brown granules) and other hepatocytes display abundant lipid droplets and few or no detectable peroxisomes. D and E, liver of an 8-month-old (D) and 12-month-old (E) AOX<sup>-/-</sup> mouse reveals a profound increase in the number of peroxisomes (brown granules) in all hepatocytes. A macrophage (D, \*) with lipid debris similar to that shown in panel B (arrows) has no peroxisome. F, wild-type (AOX<sup>+/+</sup>) mouse liver shows few peroxisomes (arrows). Erythrocytes in sinusoids (C, E, and F) show intense reaction due to the peroxidatic activity of hemoglobin.



as methyl clofenapate, Wy-14, 643, and ciprofibrate (5, 27). This magnitude of spontaneous peroxisome proliferation clearly suggests that PPAR $\alpha$  is transcriptionally activated in AOX<sup>-/-</sup> mice due to increases in the levels of biological (natural) ligands (agonists) of this transcription factor. To further affirm PPAR $\alpha$  activation, the structural findings are extended by analysis of the mRNA levels of selected genes in liver that are regulated by PPAR $\alpha$  (for review see Refs. 9, 10, and 38). As shown in Fig. 3, the remaining two genes (down-stream of AOX) of the peroxisomal  $\beta$ -oxidation system, namely MFP and THL, are up-regulated (~10–30-fold) in AOX<sup>-/-</sup> mice. The MFP mRNA level showed a remarkable increase in the liver of 2–8-month-old AOX<sup>-/-</sup> mice (Fig. 3, lanes 3–6) compared with wild-type controls (Fig. 3, lanes 1 and 2). This may be due to the presence of four imperfect TGACCT motifs in the MFP gene promoter, constituting a unique hyper-responsive PPAR-RXR heterodimer binding site (39). Significant increases in hepatic CYP4A1 and CYP4A3 mRNA levels are also discerned in AOX<sup>-/-</sup> mice (Fig. 3). These two members of the CYP4A subfamily encode microsomal fatty acid  $\omega$ -hydroxylases, and an increase in the activity of this enzyme system is a component of the peroxisome proliferator-induced pleiotropic responses in liver (7, 8). Peroxisomal membranes contain proteins, including PMP70 and X-linked adrenoleukodystrophy protein, that possibly serve as carriers for VLCFAs (40, 41). In addition ACS, which converts inactive fatty acids into active acyl-CoA derivatives, also plays a key role in peroxisomal fatty acid metabolism (42). In the liver of animals exposed to peroxisome proliferators, increases in PMP70 and ACS mRNA levels occur to reflect increases in peroxisomal membrane profiles (40, 42, 43). The mRNA levels of both ACS and PMP70 increased markedly

in the liver of AOX<sup>-/-</sup> mice, with spontaneous peroxisome proliferation (Fig. 3). The mRNA level of FAS, which catalyzes seven reactions involved in the conversion of acetyl-CoA and malonyl-CoA to palmitate (44), is also increased in the liver of 2-to-8-month-old AOX<sup>-/-</sup> mice (Fig. 3). This increase is most marked in 6- and 8-month-old mice. Modest increases in liver FABP (~3–4-fold increase), UOX (~2–4-fold), and catalase (~2-fold) mRNA levels occurred in the liver of AOX<sup>-/-</sup> mice (Fig. 3). The basal levels of these three mRNAs in wild-type mice are relatively high when compared with low basal expression of genes encoding the  $\beta$ -oxidation system, CYP4A subfamily, PMP70, ACS, and FAS (Fig. 3).

To determine whether alterations in mRNA levels of MFP, THL, PMP70, and UOX represent changes in protein concentration at the peroxisome level, localization of these proteins was investigated by immunoelectron microscopy using the protein A-gold procedure (35). The matrix of peroxisomes proliferating spontaneously in AOX<sup>-/-</sup> mouse liver revealed numerous gold particles when stained with antibodies against MFP and THL, whereas hepatic peroxisomes of normal wild-type mice displayed only a few gold particles (data not shown). UOX and PMP70 staining is localized exclusively to the crystallloid cores and to the peroxisome membranes, respectively (not illustrated). Catalase has been localized to the matrix of all peroxisomes in hepatocytes of AOX<sup>-/-</sup> mice (not shown). Immunoblot analysis of liver homogenates confirmed increases in the content of MFP, THL, UOX, and PMP70 in AOX<sup>-/-</sup> mouse liver with spontaneous peroxisome proliferation (results not shown).

**Liver Tumor Development in AOX<sup>-/-</sup> Mice**—Hepatocellular adenomas and hepatocellular carcinomas developed in



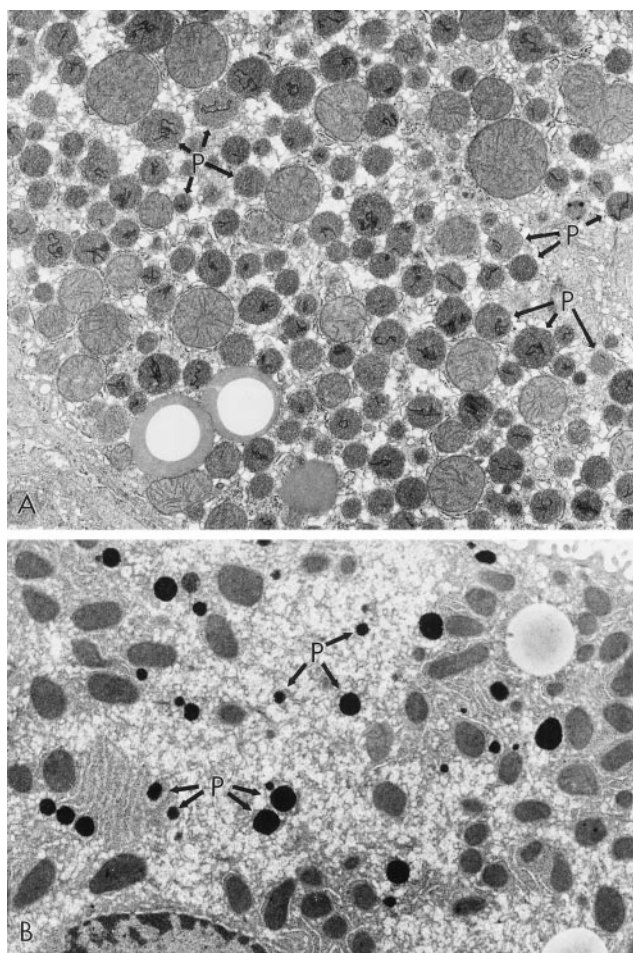


FIG. 2. Electron micrograph of a hepatocyte from the liver of an 8-month-old AOX<sup>-/-</sup> mouse (A), compared with that of a wild-type (AOX<sup>+/+</sup>) mouse (B). Liver was processed for the cytochemical localization of catalase using 3,3'-diaminobenzidine medium as described in Fig. 1. Note the presence of numerous catalase positive peroxisomes (P) with urate oxidase crystalloid inclusions in AOX<sup>-/-</sup> mouse hepatocytes. In contrast, hepatocytes in wild-type mice (A) reveal the presence of a few peroxisomes (P).

AOX<sup>-/-</sup> mice between 10 and 15 months of age (Fig. 4, A and B). By 15 months of age all AOX<sup>-/-</sup> mice developed hepatocellular carcinomas with solid, trabecular, acinar, or fibrolamellar histological patterns. No metastases to lungs or other sites were detected in AOX<sup>-/-</sup> mice killed by 15 months. Hepatic adenomas generally preceded the appearance of hepatocellular carcinomas. These adenomas and carcinomas showed reduced staining for MFP, THL, and catalase when analyzed immunohistochemically (Fig. 5). The liver parenchyma surrounding the tumors revealed a strong staining pattern for these three peroxisomal proteins. In particular, the intensity of staining was much stronger for MFP and THL (Fig. 5, C-F), the two enzymes of the  $\beta$ -oxidation system that are downstream of AOX. As expected, AOX is absent in liver and tumors in AOX<sup>-/-</sup> mice (Fig. 5A).

**Increased Hepatic H<sub>2</sub>O<sub>2</sub> Levels and Hepatocellular Regeneration**—To determine whether pronounced inflammatory response and increases in the expression of CYP4A1, CYP4A3, and possibly other enzymes in the liver of AOX<sup>-/-</sup> mice generates increased production of reactive oxygen species, the levels of H<sub>2</sub>O<sub>2</sub> in liver homogenates were measured using the phenol red method (36). In 2-month-old AOX<sup>-/-</sup>, the level of hepatic H<sub>2</sub>O<sub>2</sub> was significantly higher than that present in age-matched wild-type (AOX<sup>+/+</sup>) mice (Fig. 6A). Hepatic H<sub>2</sub>O<sub>2</sub> level was also high in 4-month-old AOX<sup>-/-</sup> mice. In 6- to 13-

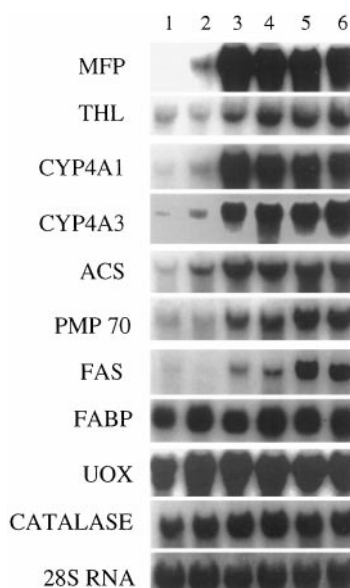


FIG. 3. Northern blot analysis of total RNA extracted from the liver of wild-type (AOX<sup>+/+</sup>) and homozygous AOX<sup>-/-</sup> mice. Lanes 1 and 2 represent control wild-type mice, and lanes 3, 4, 5, and 6 represent, respectively, 2-, 4-, 6-, and 8-month-old AOX<sup>-/-</sup> mice. Twenty  $\mu$ g of total RNA was glyoxylated, electrophoresed on a 0.8% agarose gel, blotted onto a nylon membrane, and probed with different random-primed <sup>32</sup>P-labeled cDNA probes as shown. MFP, the second gene of the peroxisomal  $\beta$ -oxidation system; THL, the third gene of the  $\beta$ -oxidation system. The 28 S RNA is for loading control.

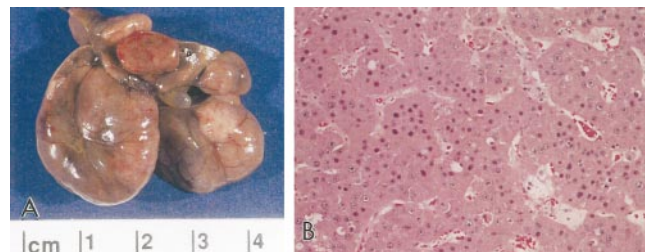


FIG. 4. Liver tumors in AOX<sup>-/-</sup> mice. The gross appearance of liver with tumors in a 14-month-old AOX<sup>-/-</sup> mice (A). Histological pattern (hematoxylin-eosin-stained) of a typical hepatocellular carcinoma in AOX<sup>-/-</sup> mice (B).

month-old AOX<sup>-/-</sup>, the levels of H<sub>2</sub>O<sub>2</sub> were elevated when compared with 2- and 13-month-old controls but not as high as in 2- to 4-month-old AOX-deficient mice (Fig. 6A). Because of the inflammatory response and isolated hepatocyte death in younger AOX<sup>-/-</sup> mice, it appeared necessary to evaluate hepatocellular proliferation in 2- to 13-month-old mice using immunohistochemical staining to localize PCNA. As shown in Fig. 6B, the most active cell proliferation occurred in the liver of AOX<sup>-/-</sup> mice between 2 to 4 months of age when compared with age-matched wild-type controls. For example, the PCNA labeling index at 4 months in AOX<sup>-/-</sup> was 5.56 as compared with 0.35 in wild-type controls. In 8- and 13-month-old AOX<sup>-/-</sup> mice, the PCNA labeling index in nontumorous areas of liver continued to be higher than that observed in controls. These observations are consistent with the proposed role of inflammatory changes, H<sub>2</sub>O<sub>2</sub> generation, and cell proliferation in carcinogenesis (45). As expected, PCNA labeling was much higher in neoplastic nodules and hepatocellular carcinomas developing in 13-month-old AOX<sup>-/-</sup> mice.

#### DISCUSSION

A variety of structurally diverse peroxisome proliferators induce predictable pleiotropic responses characterized by peroxisome proliferation and liver tumor development by a recep-



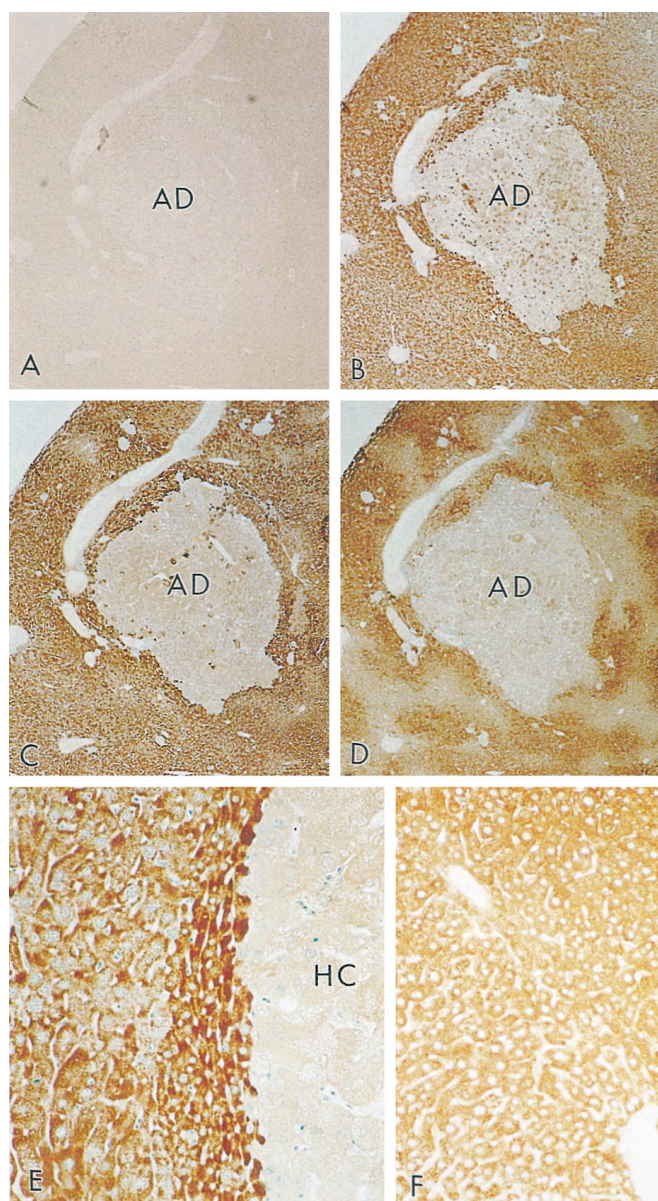


FIG. 5. Representative immunohistochemistry of liver of a 12-month-old AOX<sup>-/-</sup> mouse with a hepatic adenoma (A-D) and hepatocellular carcinoma (E). Immunoperoxidase staining for A, AOX; B, catalase; C and E, peroxisomal multifunctional protein; D, 3-ketoacyl-CoA thiolase. F, wild-type mouse (AOX<sup>+/+</sup>) stained for multifunctional protein for comparison. As expected, AOX is negative in the liver, whereas the staining for the two downstream proteins of the  $\beta$ -oxidation system is intense in nontumorous AOX<sup>-/-</sup> mouse livers. Adenomas (AD) and hepatocellular carcinomas (HC) show minimal or no staining in comparison to the surrounding liver.

tor-mediated cell-specific mechanism (4, 5, 9, 11). Recent assays based on *in vitro* binding, conformation change, or receptor-coactivator transactivation indicate that these synthetic peroxisome proliferators act as direct ligands for PPAR $\alpha$  (21, 22, 24). These studies have also shown that fatty acids, i.e. 18:2 (*n*-6), 18:3 (*n*-3 and *n*-6), and 20:4 (*n*-6), as well as the eicosanoids 8(S)-hydroxyeicosatetraenoic acid and leukotriene B<sub>4</sub>, and prostaglandin I<sub>2</sub> analogs carbaprostacyclin and iloprost function as PPAR $\alpha$  ligands (21, 22, 24). Direct activation of PPARs by fatty acids and eicosanoids is an attractive mechanism regulating lipid homeostasis. However, these natural ligands do not induce peroxisome proliferation-associated pleiotropic responses in liver cells to the same extent as those induced by synthetic ligands, such as peroxisome proliferators and 5,8,11,14-

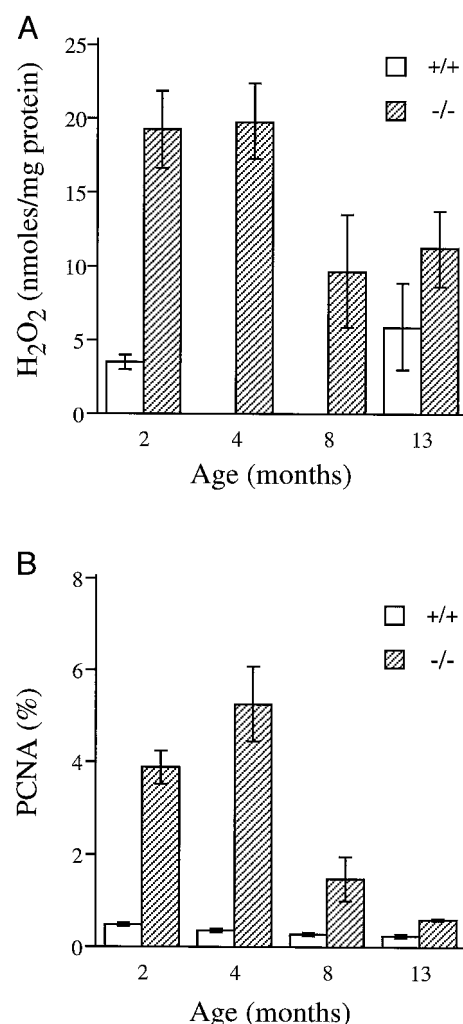
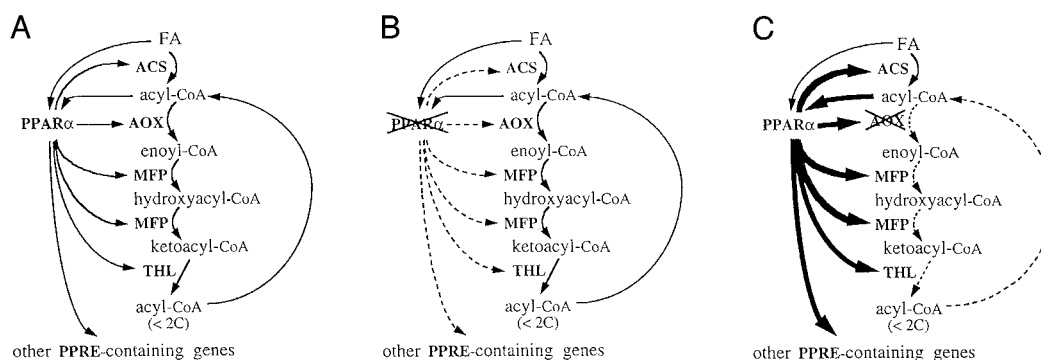


FIG. 6. H<sub>2</sub>O<sub>2</sub> level and cell proliferation index in the liver of AOX<sup>-/-</sup> mice. A, H<sub>2</sub>O<sub>2</sub> concentration in liver homogenates was determined by phenol red method. Two- to 13-month old AOX<sup>-/-</sup> mice (hatched bars) and age-matched wild-type (AOX<sup>+/+</sup>) mice (plain bars) were killed. The values are expressed as mean  $\pm$  S.E. for 3 to 4 animals for each interval. B, liver cell proliferation index was ascertained by immunoperoxidase staining of liver sections to localize PCNA. Proliferation index (percent labeling) was estimated by counting 2000 cells for each animal.

eicosatetraenoic acid, a nonmetabolizable synthetic fatty acid (24, 27). It is possible that natural fatty acids either function as weak ligands for PPAR $\alpha$  *in vivo* or that liver cells have a high capacity for  $\beta$ -oxidation, thereby preventing the accumulation of these ligands to levels that effectively activate PPAR $\alpha$ .

The results obtained from the studies of AOX mutant mice unequivocally establish the spontaneous induction of PPAR $\alpha$ -mediated pleiotropic responses, including profound peroxisome proliferation and development of liver tumors, reminiscent of those encountered in rats and mice exposed to synthetic peroxisome proliferators. In the liver of these AOX<sup>-/-</sup> mice, there is clear evidence of enhanced transcriptional activity of PPAR $\alpha$  on PPAR $\alpha$ -regulated genes. Spontaneous increases in liver mRNA levels in AOX<sup>-/-</sup> mice of MFP, PTHL, CYP4A1, CYP4A3, ACS, and PMP70 genes that have PPRE-containing promoters are comparable with those observed in the liver of wild-type mice exposed to synthetic peroxisome proliferators. Accordingly, the results of this study establish a fundamental role for AOX in the biological activities of PPAR $\alpha$  (Fig. 7). AOX, the first enzyme of the peroxisomal  $\beta$ -oxidation system, oxidizes the long chain acyl-CoA (>C<sub>20</sub>) to 2-*trans*-enoyl-CoA for



**FIG. 7. Model illustrating the role of AOX vis-à-vis acyl-CoA and other putative substrates of AOX in the activation of PPARα in normal (A), PPARα-/- (B), and AOX-/- (C) mice.** FA represents long chain and very long chain fatty acids (>C<sub>20</sub>) that are preferentially metabolized by peroxisomal β-oxidation system (31). Long chain ACS converts FA to acyl-CoA, which enters the peroxisomal β-oxidation spiral. Acyl-CoA is desaturated to a *trans*-enoyl-CoA by AOX, the first enzyme of the β-oxidation system (3). Enoyl-CoA is metabolized to hydroxyacyl-CoA and ketoacyl-CoA by the second multifunctional enzyme (MFP) of the β-oxidation system. Ketoacyl-CoA is thiololytically cleaved by thiolase (THL), the third enzyme of the β-oxidation system, to release acyl-CoA (2 carbon atoms shorter than the original molecule), which can re-enter the β-oxidation spiral, and acetyl-CoA, which can be converted in to a fatty acid by fatty acid synthase (30). In wild-type mice, PPARα is known to regulate ACS, AOX, MFP, THL, and several other target genes that possess PPRE. Recent studies dealing with transfection and transactivation indicate that fatty acids and eicosanoids are ligands for PPARα (21, 22, 24), but it is well known that fatty acids are not very efficient in inducing peroxisome proliferation *in vivo* when compared with synthetic peroxisome proliferators (27). Studies with PPARα-/- mice have unequivocally established the crucial role for this receptor in peroxisome proliferator-induced pleiotropic effects, as PPARα-/- mice failed to respond to peroxisome proliferators (25, 35). The data on the profound proliferation of peroxisomes and activation of several PPARα-responsive genes that we presented in this paper on AOX-/- mice as well as the failure of fatty acids to induce peroxisome proliferation in liver to the same extent as peroxisome proliferators strongly indicate that acyl-CoA and other natural substrates of AOX serve as the biological ligands (agonists) for PPARα. Inability of AOX-/- mice to metabolize acyl-CoA (most likely long chain and very long chain fatty acyl-CoAs) and other putative AOX ligands leads to sustained activation of PPARα and up-regulation of genes that possess PPRE.

further processing in the β-oxidation spiral (Fig. 7). VLCFAs, metabolized almost exclusively by the peroxisomal β-oxidation, must first be activated by ACS to acyl-CoA. AOX deficiency imposes a block on long chain acyl-CoA to enter the β-oxidation pathway. It is conceivable that unmetabolized long chain acyl-CoA then functions as a biological ligand of PPARα, leading to sustained transcriptional enhancement of genes with PPRE-containing promoters (Fig. 7).

It is worth noting that long chain acyl-CoA was once considered a metabolic message responsible for the induction of β-oxidation system (46, 47). This raises the issue whether free fatty acids and unmetabolized synthetic peroxisome proliferators act as direct ligands of PPARα *in vivo* or that activation of this receptor is mediated by their CoA esters and other downstream derivatives resulting from the β-oxidation. The sulfur-substituted fatty acid derivatives and peroxisome proliferators of the fibrate class are activated to their esters with CoA. Although these cannot enter the β-oxidation spiral, they can still function efficiently as peroxisome proliferators *in vivo*, implying that β-oxidation is not essential to generate the PPARα agonists (47, 48). In X-linked adrenoleukodystrophy (X-ALD), a peroxisomal disorder with impaired VLCFA metabolism, there is progressive VLCFA accumulation, resulting in neurological abnormalities and death during childhood (32, 41). In X-ALD patients, there is no report of spontaneous peroxisome proliferation in liver parenchymal cells despite VLCFA accumulation (32, 41). This lack of peroxisome proliferation in X-ALD patients may not be attributable entirely to differences in the sensitivity of human PPARα (49), because there is no indication of the occurrence of spontaneous peroxisome proliferation in mouse models for this disease, developed recently by inactivating X-ALD gene (50, 51). In addition, failure to induce peroxisome proliferation by dietary lipid overload (27, 52) and by increased VLCFA levels in X-ALD (32, 41, 50, 51) implies that, under *in vivo* conditions, fatty acids are not effective inducers of PPARα. In contrast, the remarkable induction of spontaneous peroxisome proliferative response in AOX null mice raises the possibility that the PPARα signal-transducing event is distal to the ACS-catalyzed fatty acid activation step (Fig. 7). In this context it is important to note that fatty acyl-

CoAs have been shown to act as potent inhibitors of the nuclear thyroid hormone receptor and promoted dissociation of the hormone bound to the receptor (53). Long chain fatty acids are activated by ACS to their corresponding acyl-CoAs, which either participate in the synthesis of cellular lipids including triacylglycerols, phospholipids, and cholesterol esters or enter the peroxisomal β-oxidation spiral for degradation (3, 30). The strong increases of hepatic ACS mRNA in AOX-/- mice (Fig. 3) suggests efficient VLCFA activation to acyl-CoA, but the resulting acyl-CoA cannot be β-oxidized by peroxisomes due to lack of AOX in these mice. The observed increases in ACS mRNA and PPARα activation in AOX-/- mice do not support the possibility that ACS may inactivate PPARα ligands (21). However, quantitative data on the levels of VLCFAs and fatty acyl-CoAs are necessary to provide direct evidence for the efficient conversion of VLCFAs to acyl-CoAs in AOX-/- mouse liver. It is also important to consider the possibility that long chain acyl-CoA thioesterases may play an active role in cleaving fatty acyl-CoA to the corresponding free fatty acids and CoASH (54, 55) and, thus, modulate the levels of acyl-CoAs in AOX-/- mouse liver. Since these thioester hydrolases in rat liver are inducible by peroxisome proliferators (55), it would be important to determine the levels of these enzymes in AOX-/- mouse liver to appreciate the relative importance of free VLCFAs and their CoA derivatives in the activation *in vivo* of PPARα. Recently, the eicosanoids 8(S)-hydroxyeicosatetraenoic acid and leukotriene B<sub>4</sub>, which are derived from arachidonic acid, have also been shown to function as ligands for PPARα (21, 22, 24, 56). Since leukotriene B<sub>4</sub> is β-oxidized within the peroxisome (57, 58), there is a possibility that these endogenous ligands of PPARα may also contribute to enhanced PPARα activation in the liver of AOX-/- mice. Nonetheless, the data presented here clearly establish that a functional AOX gene is a key regulator of PPARα function by its ability to metabolize acyl-CoA vis-à-vis fatty acids and thus keep the level of these and other physiological PPARα ligands in check. Thus, this mouse model of peroxisomal AOX deficiency may provide helpful clues in the search for the PPARα agonists and in screening for the antagonists for this receptor.

Massive increases in the levels of ACS, MFP, THL, CYP4A1,



and CYP4A3 mRNAs in the liver of AOX<sup>-/-</sup> mice reflect spontaneous induction of the PPAR $\alpha$  signal transduction pathway, affecting a plethora of genes with PPRE-containing promoters (Fig. 7). The induction in AOX<sup>-/-</sup> mice of PPAR $\alpha$ -mediated pleiotropic responses, including the development of liver tumors, strongly implies that PPAR $\alpha$  functions as an oncogene in liver. The abrogation of peroxisome proliferator-induced pleiotropic responses including the development of liver tumors in PPAR $\alpha$  <sup>-/-</sup> mice supports this contention (37). This interpretation is consistent with our proposal more than a decade ago that the receptor-mediated activation of specific genes and peroxisome proliferation-induced oxidative stress lead to oncogenesis in liver (27, 28). We further propose that AOX gene functions as a tumor suppressor gene under normal physiological conditions by metabolizing PPAR $\alpha$  ligands. Our data also indicate that inactivation of tumor suppressor function of AOX gene leads to oncogenesis. The suggestion that normal AOX functions as a tumor suppressor gene may appear paradoxical, because increased AOX activity in rats and mice exposed to peroxisome proliferators results in excess production of H<sub>2</sub>O<sub>2</sub>, leading to sustained oxidative stress, thus contributing to liver tumor development (5, 27, 28). The precise mechanism by which AOX null mice, which show extensive spontaneous peroxisome proliferation, develop liver tumors, remains to be elucidated. It is important to point out that these animals, during steatotic phase, exhibited marked inflammatory response, increased hepatic levels of H<sub>2</sub>O<sub>2</sub>, and hepatocellular proliferation. Proinflammatory molecules such as leukotriene B<sub>4</sub> and 8(S)-hydroxyeicosatetraenoic acid are normally degraded by the peroxisomal  $\beta$ -oxidation system, and the ineffective degradation of these agents in AOX<sup>-/-</sup> mice may lead to inflammatory changes. Inflammatory cell infiltrate, as well as increased levels of CYP4A1 and CYP4A3 are known to generate reactive oxygen species and can lead to oxidative DNA damage similar to that observed in the livers of rats and mice exposed to peroxisome proliferators (45). Cell proliferation occurring in these livers of AOX<sup>-/-</sup> mice can facilitate the fixation of resulting mutations. In AOX<sup>-/-</sup> mice, putative preneoplastic and neoplastic liver lesions manifested between 10 and 15 months of age, which essentially paralleled the changes observed in wild-type rats and mice exposed to peroxisome proliferators (5, 26, 28). Our findings suggest that AOX-deficient mice will be an invaluable model system for the further unraveling of the molecular events in PPAR $\alpha$ -mediated signal transduction, hepatitis, liver cell regeneration, and oncogenesis.

**Acknowledgments**—We thank H. Sakuraba for assisting with mouse colony, Sujatha Pulikuri for excellent technical assistance, and Vanessa Jones for the preparation of illustrations. We are grateful to Dr. J. I. Gordon for the liver FABP plasmid, to Dr. Frank J. Gonzalez for CYP4A1 and CYP4A3 plasmids, to Drs. Genevieve Martin and Johan Auwerx for the ACS plasmid, to Dr. Takashi Hashimoto for PMP70 plasmid, and to Dr. D. B. Jump for the FAS plasmid.

## REFERENCES

- De Duve, C. (1996) *Ann. N. Y. Acad. Sci.* **804**, 1–10
- Tolbert, N. E. (1981) *Annu. Rev. Biochem.* **50**, 133–157
- Reddy, J. K., and Mannaerts, G. P. (1994) *Annu. Rev. Nutr.* **14**, 343–370
- Reddy, J. K., and Krishnakantha, T. P. (1975) *Science* **200**, 787–789
- Reddy, J. K., and Lalwani, N. D. (1983) *CRC Crit. Rev. Toxicol.* **12**, 1–58
- Lazarow, P. B., and De Duve, C. (1976) *Proc. Natl. Acad. Sci. U. S. A.* **73**, 2043–2046
- Reddy, J. K., Goel, S. K., Nemali, M. R., Carrino, J. J., Laffler, T. G., Reddy, M. K., Sperbeck, S. J., Osumi, T., Hashimoto, S., Lalwani, N. D., and Rao, M. S. (1986) *Proc. Natl. Acad. Sci. U. S. A.* **83**, 1747–1751
- Johnson, E. F., Palmer, C. N. A., Groffin, K. J., and Hsu, M.-H. (1996) *FASEB J.* **10**, 1241–1248
- Reddy, J. K., and Chu, R. (1996) *Ann. N. Y. Acad. Sci.* **804**, 176–201
- Lemberger, T., Desvergne, B., and Wahli, W. (1996) *Annu. Rev. Cell Dev. Biol.* **12**, 335–363
- Isseimann, I., and Green, S. (1990) *Nature* **347**, 645–650
- Kliwer, S. A., Umesono, K., Noonan, D. J., Heyman R. A., and Evans, R. M. (1992) *Nature* **358**, 771–774
- Dreyer, C., Krey, G., Keller, H., Givel, F., Helftenbein, G., and Wahli, W. (1992) *Cell* **68**, 879–887
- Zhu, Y., Alvares, K., Huang, Q., Rao, M. S., and Reddy, J. K. (1993) *J. Biol. Chem.* **268**, 26817–26820
- Kliwer, S. A., Forman, B. M., Blumberg, B., Ong, E. S., Borgmeyer, U., Mangelsdorf, D. J., Umesono, K., and Evans, R. M. (1994) *Proc. Natl. Acad. Sci. U. S. A.* **91**, 7355–7359
- Sher, T., Yi, H. F., McBride, W., and Gonzalez, F. J. (1993) *Biochemistry* **32**, 5598–5604
- Huang, Q., Yeldandi, A. V., Alvares, K., Ide, H., Reddy, J. K., and Rao, M. S. (1995) *Int. J. Oncol.* **6**, 307–312
- Braissant, O., Fougelle, F., Scotto, C., Dauca, M., and Wahli, W. (1996) *Endocrinology* **137**, 354–366
- Zhu, Y., Qi, C., Korenberg, J. R., Chen, X.-N., Noya, D., Rao, M. S., and Reddy, J. K. (1995) *Proc. Natl. Acad. Sci. U. S. A.* **92**, 7921–7925
- Gottlicher, M., Widmark, E., Li, Q., and Gustafsson, J. A. (1992) *Proc. Natl. Acad. Sci. U. S. A.* **89**, 4653–4657
- Forman, B. M., Chen, J., and Evans, R. M. (1997) *Proc. Natl. Acad. Sci. U. S. A.* **94**, 4312–4317
- Kliwer, S. A., Sundseth, S. S., Jones, S. A., Brown, P. J., Wisely, G. B., Koble, C. S., Devchand, P., Wahli, W., Wilson, T. M., Lenhard, J. M., and Lehman, J. M. (1997) *Proc. Natl. Acad. Sci. U. S. A.* **94**, 4318–4323
- Forman, B. M., Tontonoz, P., Chen, J., Brun, R. P., Spiegelman, B. M., and Evans, R. M. (1995) *Cell* **83**, 803–812
- Krey, G., Braissant, O., L'Horsset, F., Kalkhoven, E., Perroud, M., Parker, M. G., and Wahli, W. (1997) *Mol. Endocrinol.* **11**, 779–791
- Lee, S.-T., Pineau, T., Drago, J., Lee, E. J., Owens, J. W., Kroetz, D. L., Fernandez-Salguero, P. M., Westphal, H., and Gonzalez, F. J. (1995) *Mol. Cell. Biol.* **15**, 3012–3022
- Reddy, J. K., Azarnoff, D. L., and Hignite, C. F. (1980) *Nature* **283**, 397–398
- Reddy, J. K., and Rao, M. S. (1986) *Trends Pharmacol. Sci.* **7**, 438–443
- Rao, M. S., and Reddy, J. K. (1987) *Carcinogenesis* **8**, 631–636
- Ashby, J., Brady, A., Elcombe, C. R., Elliot, B. M., Ishmael, J., Odum, J., Tugwood, J. D., Kettle, S., and Purchase, L. F. H. (1994) *Hum. Exp. Toxicol.* **13**, Suppl. 2, 1–117
- Hashimoto, T. (1996) *Ann. N. Y. Acad. Sci.* **804**, 86–98
- Singh, I., Moser, A. E., Goldfischer, S., and Moser, H. W. (1984) *Proc. Natl. Acad. Sci. U. S. A.* **81**, 4203–4207
- Lazarow, P. B., and Moser, H. W. (1995) in *The Metabolic Basis of Inherited Disease* (Scriver, C. R., Beaudet, A. L., Sly, W. S., and Valle, A. D., eds) pp. 2287–2324, McGraw-Hill, New York
- Poll-The, B. T., Saudubray, J. M., Ogier, H., Schutgens, R. B. H., Wanders, R. J. A., Schramkamp, G., Van den Bosch, H., Trybels, J. M. F., Poulos, A., Moser, H. W., van Eldere, J., Eyssen, H. J. (1987) *Eur. J. Pediatr.* **146**, 477–483
- Fan, C.-Y., Pan, J., Chu, R., Lee, D., Kluckman, K. D., Usuda, N., Singh, I., Yeldandi, A. V., Rao, M. S., Maeda, N., and Reddy, J. K. (1996) *J. Biol. Chem.* **271**, 24698–24710
- Usuda, N., Nakazawa, A., Terasawa, M., Reddy, J. K., and Nagata, T. (1996) *Ann. N. Y. Acad. Sci.* **804**, 297–309
- Pick, E., and Keisari, Y. (1980) *J. Immunol. Methods* **38**, 161–170
- Peters, J. M., Cattley, R. C., and Gonzalez, F. J. (1987) *Carcinogenesis* **18**, 2029–2033
- Schoonjans, K., Staels, B., and Auwerx, J. (1996) *J. Lipid Res.* **37**, 907–925
- Chu, R., Lin, Y., Rao, M. S., and Reddy, J. K. (1995) *J. Biol. Chem.* **270**, 29636–29639
- Kamijo, K., Taketani, S., Yokota, S., Osumi, T., and Hashimoto, T. (1990) *J. Biol. Chem.* **265**, 4534–4540
- Mosser, J., Douar, A.-M., Sarde, C.-O., Kioschis, P., Feil, R., Moser, H., Poustka, A.-M., Mandel, J.-L., and Aubourg, P. (1993) *Nature* **361**, 726–730
- Schoonjans, K., Watanabe, M., Suzuki, H., Mahfoudi, A., Krey, G., Wahli, W., Grimaldi, P., Staels, B., Yamamoto, T., and Auwerx, J. (1995) *J. Biol. Chem.* **270**, 19269–19276
- Martin, G., Schoonjans, K., Lefebvre, A.-M., Staels, B., and Auwerx, J. (1997) *J. Biol. Chem.* **272**, 28210–28217
- Paulauskis, J. D., and Sul, H. S. (1988) *J. Biol. Chem.* **263**, 7049–7054
- Ames, B. N., Gold, L. S., and Willett, W. C. (1995) *Proc. Natl. Acad. Sci. U. S. A.* **92**, 5258–5265
- Berge, R. K., and Aarsland, A. (1985) *Biochim. Biophys. Acta* **837**, 141–151
- Gottlicher, M., Demoz, A., Svensson, D., Tollet, P., Berge, R. K., and Gustafsson, J.-A. (1993) *Biochem. Pharmacol.* **46**, 2177–2184
- Aarsland, A., and Berge, R. K. (1991) *Biochem. Pharmacol.* **41**, 53–61
- Tugwood, J. D., Alridge, T. C., Lambe, K. G., MacDonald, N., and Woodyatt, N. J. (1996) *Ann. N. Y. Acad. Sci.* **804**, 252–265
- Lu, J.-F., Lawler, A. M., Watkins, P. A., Powers, J. M., Moser, A. B., Moser, H. W., and Smith, K. D. (1997) *Proc. Natl. Acad. Sci. U. S. A.* **94**, 9366–9371
- Kobayashi, T., Shinonoh, N., Kondo, A., and Yamada, T. (1997) *Biochem. Biophys. Res. Commun.* **232**, 631–636
- Ren, B., Thelen, A. P., Peters, J. M., Gonzalez, F. J., and Jump, D. B. (1997) *J. Biol. Chem.* **272**, 26827–26832
- Li, Q., Yamamoto, N., Inoue, A., and Morisawa, S. (1990) *J. Biochem. (Tokyo)*, **107**, 699–702
- Svensson, L. T., Wilcke, M., and Alexson, S. E. H. (1995) *Eur. J. Biochem.* **230**, 813–820
- Broustas, C. G., Larkins, L. K., Uhler, M. D., and Hajra, A. K. (1996) *J. Biol. Chem.* **271**, 10470–10476
- Yu, K., Bayona, W., Kallen, C. B., Harding, H. P., Ravera, C. P., McMahon, G., Brown, M., and Lazar, M. A. (1995) *J. Biol. Chem.* **270**, 23975–23983
- Furstenberger, G., Hagedorn, H., Jacobi, T., Besemfelder, E., Stephan, M., Lehmann, W.-D., and Marks, F. (1991) *J. Biol. Chem.* **266**, 15738–15745
- Devchand, P. R., Keller, H., Peters, J. M., Vazquez, M., Gonzalez, F. J., and Wahli, W. (1996) *Nature* **384**, 39–43